



University of Pennsylvania
ScholarlyCommons

Departmental Papers (CBE)

Department of Chemical & Biomolecular
Engineering

6-1-2007

Micelles of Different Morphologies - Advantages of Worm-like Filomicelles of PEO-PCL in Paclitaxel Delivery

Shenshen Cai
University of Pennsylvania

Kandaswamy Vijayan
University of Pennsylvania

Debbie Cheng
University of Pennsylvania

Eliana M. Lima
University of Pennsylvania

Dennis E. Discher
University of Pennsylvania, discher@seas.upenn.edu

Follow this and additional works at: http://repository.upenn.edu/cbe_papers

 Part of the [Biochemical and Biomolecular Engineering Commons](#)

Recommended Citation

Cai, S., Vijayan, ., Cheng, D., Lima, E. M., & Discher, D. E. (2007). Micelles of Different Morphologies - Advantages of Worm-like Filomicelles of PEO-PCL in Paclitaxel Delivery. Retrieved from http://repository.upenn.edu/cbe_papers/91

Preprint version. Published in *Pharmaceutical Research*, Volume 24, Issue 6, June 2007, 14 pages.
Publisher URL: 10.1007/s11095-007-9335-z

This paper is posted at ScholarlyCommons. http://repository.upenn.edu/cbe_papers/91
For more information, please contact libraryrepository@pobox.upenn.edu.

Micelles of Different Morphologies - Advantages of Worm-like Filomicelles of PEO-PCL in Paclitaxel Delivery

Abstract

Worm-like and spherical micelles are both prepared here from the same amphiphilic diblock copolymer, poly(ethylene oxide)-*b*-poly(ϵ -caprolactone) (PEO [5 kDa]-PCL [6.5 kDa]) in order to compare loading and delivery of hydrophobic drugs. Worm-like micelles of this degradable copolymer are nanometers in cross-section and spontaneously assemble to stable lengths of microns, resembling filoviruses in some respects and thus suggesting the moniker "filomicelles". The highly flexible worm-like micelles can also be sonicated to generate kinetically stable spherical micelles composed of the same copolymer. The fission process exploits the finding that the PCL cores are fluid, rather than glassy or crystalline, and core-loading of the hydrophobic anticancer drug delivery, paclitaxel (TAX) shows that the worm-like micelles load and solubilize twice as much drug as spherical micelles. In cytotoxicity tests that compare to the clinically prevalent solubilizer, Cremophor® EL, both micellar carriers are far less toxic, and both types of TAX-loaded micelles also show 5-fold greater anticancer activity on A549 human lung cancer cells. PEO-PCL based worm-like filomicelles appear to be promising pharmaceutical nanocarriers with improved solubilization efficiency and comparable stability to spherical micelles, as well as better safety and efficacy *in vitro* compared to the prevalent Cremophor® EL TAX formulation.

Keywords

lung carcinoma cells, paclitaxel, poly(epsilon-caprolactone), poly(ethylene oxide), worm-like micelle

Disciplines

Biochemical and Biomolecular Engineering

Comments

Preprint version. Published in *Pharmaceutical Research*, Volume 24, Issue 6, June 2007, 14 pages.

Publisher URL: [10.1007/s11095-007-9335-z](http://dx.doi.org/10.1007/s11095-007-9335-z)

Metadata of the article that will be visualized in OnlineFirst

| | | | |
|----|----------------------|--|---|
| 1 | Article Title | Micelles of Different Morphologies—Advantages of Worm-like Filomicelles of PEO-PCL in Paclitaxel Delivery | |
| 2 | Journal Name | Pharmaceutical Research | |
| 3 | | Family Name | Discher |
| 4 | | Particle | |
| 5 | | Given Name | Dennis E. |
| 6 | Corresponding Author | Suffix | |
| 7 | | Organization | University of Pennsylvania Philadelphia |
| 8 | | Division | Department of Chemical and Biomolecular Engineering |
| 9 | | Address | Pennsylvania 19104, USA |
| 10 | | e-mail | discher@seas.upenn.edu |
| 11 | | Family Name | Cai |
| 12 | | Particle | |
| 13 | | Given Name | Shenshen |
| 14 | | Suffix | |
| 15 | Author | Organization | University of Pennsylvania Philadelphia |
| 16 | | Division | Department of Chemical and Biomolecular Engineering |
| 17 | | Address | Pennsylvania 19104, USA |
| 18 | | e-mail | |
| 19 | | | Family Name |
| 20 | | Particle | |
| 21 | | Given Name | Kandaswamy |
| 22 | | Suffix | |
| 23 | Author | Organization | University of Pennsylvania Philadelphia |
| 24 | | Division | Department of Chemical and Biomolecular Engineering |
| 25 | | Address | Pennsylvania 19104, USA |
| 26 | | e-mail | |
| 27 | | | Family Name |
| 28 | | Particle | |
| 29 | | Given Name | Debbie |
| 30 | | Suffix | |
| 31 | Author | Organization | University of Pennsylvania Philadelphia |
| 32 | | Division | Department of Chemical and Biomolecular Engineering |
| 33 | | Address | Pennsylvania 19104, USA |
| 34 | | e-mail | |
| 35 | | | Family Name |

| | | |
|----|-----------------------------|---|
| | | Lima |
| 36 | Particle | |
| 37 | Given Name | Eliana M. |
| 38 | Suffix | |
| 39 | Author | |
| | Organization | University of Pennsylvania Philadelphia |
| 40 | Division | Department of Chemical and Biomolecular Engineering |
| 41 | Address | Pennsylvania 19104, USA |
| 42 | e-mail | |
| 43 | Received | 10 April 2007 |
| 44 | Schedule | Revised |
| 45 | Accepted | 2 May 2007 |
| 46 | Abstract | <p>Worm-like and spherical micelles are both prepared here from the same amphiphilic diblock copolymer, poly(ethylene oxide)-<i>b</i>-poly(ϵ-caprolactone) (PEO [5 kDa]-PCL [6.5 kDa]) in order to compare loading and delivery of hydrophobic drugs. Worm-like micelles of this degradable copolymer are nanometers in cross-section and spontaneously assemble to stable lengths of microns, resembling filoviruses in some respects and thus suggesting the moniker 'filomicelles'. The highly flexible worm-like micelles can also be sonicated to generate kinetically stable spherical micelles composed of the same copolymer. The fission process exploits the finding that the PCL cores are fluid, rather than glassy or crystalline, and core-loading of the hydrophobic anticancer drug delivery, paclitaxel (TAX) shows that the worm-like micelles load and solubilize twice as much drug as spherical micelles. In cytotoxicity tests that compare to the clinically prevalent solubilizer, Cremophor® EL, both micellar carriers are far less toxic, and both types of TAX-loaded micelles also show 5-fold greater anticancer activity on A549 human lung cancer cells. PEO-PCL based worm-like filomicelles appear to be promising pharmaceutical nanocarriers with improved solubilization efficiency and comparable stability to spherical micelles, as well as better safety and efficacy <i>in vitro</i> compared to the prevalent Cremophor® EL TAX formulation.</p> |
| 47 | Keywords separated by ' - ' | lung carcinoma cells - paclitaxel - poly(ϵ -caprolactone) - poly(ethylene oxide) - worm-like micelle |
| 48 | Foot note information | |

Research Paper

1
2 **Micelles of Different Morphologies—Advantages of Worm-like Filomicelles**
3 **of PEO-PCL in Paclitaxel Delivery**4 **Shenshen Cai,¹ Kandaswamy Vijayan,¹ Debbie Cheng,¹ Eliana M. Lima,¹ and Dennis E. Discher^{1,2}**5 *Received April 10, 2007; accepted May 2, 2007*

6 **Abstract.** Worm-like and spherical micelles are both prepared here from the same amphiphilic diblock
7 copolymer, poly(ethylene oxide)-*b*-poly (ϵ -caprolactone) (PEO [5 kDa]-PCL [6.5 kDa]) in order to
8 compare loading and delivery of hydrophobic drugs. Worm-like micelles of this degradable copolymer
9 are nanometers in cross-section and spontaneously assemble to stable lengths of microns, resembling
10 filoviruses in some respects and thus suggesting the moniker 'filomicelles'. The highly flexible worm-like
11 micelles can also be sonicated to generate kinetically stable spherical micelles composed of the same
12 copolymer. The fission process exploits the finding that the PCL cores are fluid, rather than glassy or
13 crystalline, and core-loading of the hydrophobic anticancer drug delivery, paclitaxel (TAX) shows that
14 the worm-like micelles load and solubilize twice as much drug as spherical micelles. In cytotoxicity tests
15 that compare to the clinically prevalent solubilizer, Cremophor® EL, both micellar carriers are far less
16 toxic, and both types of TAX-loaded micelles also show 5-fold greater anticancer activity on A549
17 human lung cancer cells. PEO-PCL based worm-like filomicelles appear to be promising pharmaceutical
18 nanocarriers with improved solubilization efficiency and comparable stability to spherical micelles, as
19 well as better safety and efficacy *in vitro* compared to the prevalent Cremophor® EL TAX formulation.

21 **KEY WORDS:** lung carcinoma cells; paclitaxel; poly(ϵ -caprolactone); poly(ethylene oxide);
22 worm-like micelle.

24 **INTRODUCTION**

25 Parenteral delivery of chemotherapeutics is a cornerstone
26 of clinical cancer treatment, but many drugs are hydrophobic
27 and require a solubilizing carrier. Such systems must load and
28 stably retain anticancer drugs and must also have a means to
29 release drugs into cells. Anticancer drug delivery systems have
30 thus far included bioconjugates (1–3), nanoparticles (4,5),
31 liposomes (6,7), polymersomes (8–10), and polymeric micelles
32 composed of amphiphilic block copolymers (11,12), but all of
33 the cited carriers are essentially spherical in shape. Long and
34 flexible “worm-like” micelle carriers made from amphiphilic
35 block copolymers are described here in terms of formulation
36 and *in vitro* delivery, and the findings follow up on recent
37 studies that demonstrate surprisingly persistent circulation and
38 potent anti-tumor activity of worm-like micelles *in vivo* (13).

39 Paclitaxel (TAX) is a clinically prevalent anticancer agent
40 used against a variety of solid tumors (14–17), and it works by
41 stabilizing microtubules and inhibiting cytoskeleton-mediated
42 processes such as mitosis (18). However, the extremely low
43 water solubility of TAX at 0.3 $\mu\text{g/ml}$ (25°C) (18) or 3–4 $\mu\text{g/ml}$
44 at 37°C (19) has motivated both covalent modifications to
45 increase solubility (20) as well as loading into various types of
46 carrier systems. As the most common emulsifying agent used

in the clinic to solubilize TAX, Cremophor® EL is a complex, 47
viscous mixture composed primarily of hydrophobic glycer- 48
olpolyoxyethylene ricinoleates, various fatty acid esters, and 49
~50% ethanol (21,22), but clinical problems associated with 50
Cremophor EL include low drug stability after dilution in 51
aqueous medium (23) and severe, dose-limiting side effects 52
such as hypersensitivity and cardiotoxicity (20,24,25). There is 53
therefore a need for safer and more effective TAX delivery 54
systems. 55

Amphiphilic diblock copolymers generally self-assemble 56
in dilute aqueous solution into three basic morphologies: 57
spherical micelles, worm-like micelles, and vesicles. Spherical 58
micelles form spontaneously when the hydrophilic, corona 59
block such as poly(ethylene oxide) (PEO) is the largest block 60
by mass, and these have now been widely studied in bio- 61
application. Following parental administration, such spheres 62
delay clearance by macrophages of the liver and spleen due 63
to the hydrated corona and also—it has been thought—due 64
to their small size (26). Escape from clearance in principle 65
allows accumulation in tumors, and use of copolymers that 66
are degradable (27,28) or sensitive to temperature or pH can 67
provide mechanisms for controlled drug release (18,24,29). 68
By decreasing the weight fraction of the PEO block to just 69
less than ~50%, hydration and swelling of the corona imparts 70
just enough curvature to the copolymer assembly that worm- 71
like micelles that are microns in length and similar in 72
diameter to the spheres are the predominant morphology 73
for a variety of diblock copolymers (30,31). Drugs such as 74
TAX and various hydrophobic dyes have now been loaded 75

¹Department of Chemical and Biomolecular Engineering, University
of Pennsylvania Philadelphia, Pennsylvania, 19104, USA.

²To whom correspondence should be addressed. (e-mail: discher@
seas.upenn.edu)

76 into these novel carriers (30,32–34), and worm-like micelles
 77 *in vivo* persist for up to 1 week in the blood circulation,
 78 which appears longer than any other synthetic particle,
 79 including stealthy vesicles bearing the same length of PEO
 80 chains (13). In some sense, the worm-like micelles are bio-
 81 inspired by filoviruses that can also circulate and infect
 82 human cells, which is why the micelles are hereafter referred
 83 to as filomicelles.

84 In this study, worm-like filomicelles and spherical
 85 micelles were both prepared from the same poly (ethylene
 86 oxide)-*b*-poly (ϵ -caprolactone) (PEO-PCL, denoted OCL) as

sketched in Fig. 1a. Drug loading capacities were then
 directly compared, and show that approximately 2-fold
 higher TAX loading is possible with worm-like filomicelles.
 For both systems, TAX release is similarly enhanced at lower
 pH, which is favorable as cancerous tissues are generally
 associated with acidic environment (29,35). Compared to
 Cremophor EL, both polymeric micelle carriers show signifi-
 cantly less cytotoxicity and greater potency in delivering
 TAX to human lung carcinoma A549 cells. OCL-based
 worm-like filomicelles thus appear to be a promising new
 system for drug delivery.

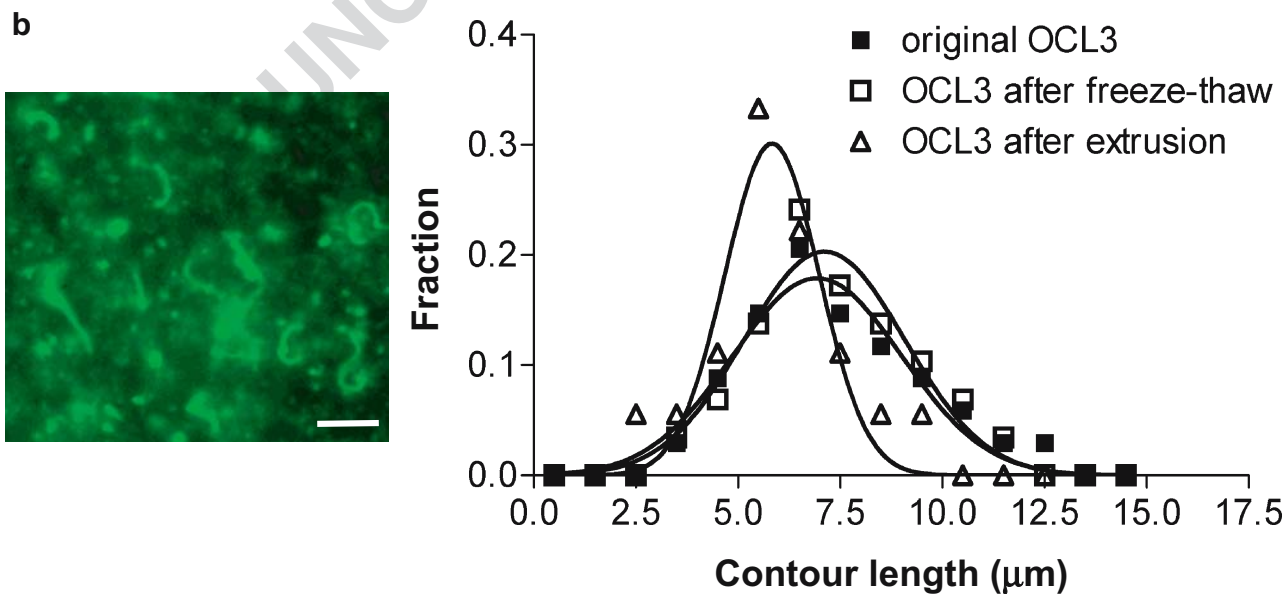
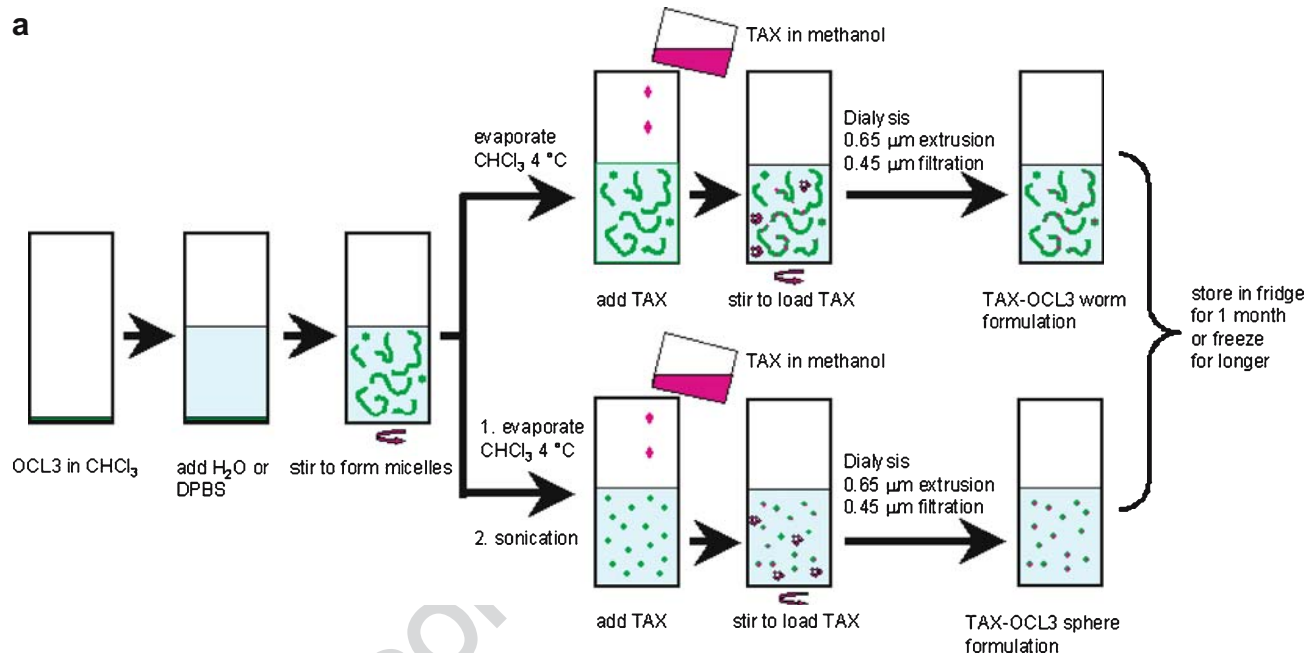


Fig. 1. Preparation of OCL3 polymeric micelles. **a** Scheme of making OCL3 micelles in worm-like and spherical morphologies; **b** visualization of worm-like micelles under fluorescence microscopy (left) and the contour length distribution of worm-like micelles, inset showing an enlarged worm-like micelle (right). Scale bar 5 μm

Micelles of Different Morphologies—Advantages of Worm-like Filomicelles of PEO-PCL in Paclitaxel Delivery98 **MATERIALS AND METHODS**99 **Materials**

100 Diblock polymer poly (ethylene oxide)-*b*-poly (ϵ -caprolactone)
101 ($M_n=5,000-6,500$, weight fraction of PEO $f_{EO}=0.43$, polydispersity=
102 1.3, denoted OCL3) was purchased from Polymersource
103 (Dorval, Canada). Paclitaxel (TAX), docetaxel, Cremophor
104 EL, fluorescent PKH26 dye, Dulbecco's phosphate-buffered
105 saline (DPBS) and methylthiazolyldiphenyl-tetrazolium
106 bromide (MTT) were from Sigma (St. Louis, MO). Human
107 lung carcinoma cells A549 were obtained from ATCC
108 (Manassas, VA). F12 Ham media was purchased from
109 Mediatech (Herndon, VA). All organic solvents were
110 analytical grade from Fisher Scientific.

111 **Preparation of OCL3 Polymeric Micelles by Cosolvent/
112 Evaporation Method**

113 The preparation of OCL3 polymeric micelles was shown
114 in Fig. 1a. Briefly, 50 μ l of 50 mg/ml OCL3 stock solution in
115 chloroform was mixed with 5 ml of water and the mixture
116 was stirred vigorously at room temperature for 1 h. Chloro-
117 form was completely removed by evaporation at 4°C for
118 overnight to obtain the final solution containing OCL3
119 worm-like micelles. Solutions at other concentrations were
120 made by varying the volume of OCL3 stock solution mixed
121 with water. OCL3 spherical micelles were obtained by
122 sonicating the worm-like micelles using Fisher 60 Sonic
123 Dismembrator equipped with Fisher Ultrasonic Converter
124 (Fisher Scientific) for 25 pulses at 1 s/pulse. All solutions
125 containing OCL3 polymeric micelles were stored at 4°C to
126 minimize degradation.

127 **Fluorescence Microscopy and Micelle Morphology Studies**

128 PKH26, which is a rhodamine-based hydrophobic fluores-
129 cent dye, was added to OCL3 micelle solutions at about 1 μ l/1 mg
130 polymer and vortexed for 10 s. The dye rapidly distributed into
131 the hydrophobic core of the micelles so the morphology of
132 micelles was visualized. Olympus IX71 inverted fluorescence
133 microscope equipped with a 60 \times objective lens and a Cascade
134 CCD camera was used to observe the micelles. About 25
135 images were taken for each sample tested and the contour
136 length of worm-like micelles was measured using Image-Pro
137 Plus (MediaCybernetics, Silver Spring, MD).

138 **Dynamic Light Scattering**

139 The average hydrodynamic micelle sizes and size distribution
140 were analyzed by dynamic light scattering (DLS) using Protein
141 Solutions™ Temperature Controlled MicroSampler and Protein
142 Solutions Dynapro™ Titan (Wyatt Technologies, Santa Barbara,
143 CA) at 25°C. The laser wavelength was 782.4 nm and the
144 scattering angle was 90°. Each sample was measured in triplicate.

145 **Crystallinity Analysis**

146 Polycaprolactone is a highly crystalline polymer in bulk.
147 In an attempt to look for crystallization at nano-scale, an
148 alternate protocol was developed that could exploit the

melting and annealing of the PCL core. Thus a 10 mg/ml stock 149
solution of OCL3 was prepared in chloroform and 15–20 μ l of 150
this stock was added to 1 ml water in a glass vial. The vial was 151
closed, briefly vortexed, and allowed to stand at room 152
temperature for 2 h. Next, the vial was incubated at 60°C with 153
the cap open, for 2 h to evaporate the chloroform in the 154
solution. The vial was then allowed to incubate at 30°C for 4–6 h. 155
Glycerol was added to the worms to make a 50% glycerol 156
solution, which was incubated at –20°C for up to 24 h. The 157
rigidity of OCL3 worms was determined by fluorescence image 158
analysis as described in “Fluorescence Microscopy and Micelle 159
Morphology Studies.” 160

The fluidity of the worm micelle core was estimated by 161
measuring the fluorescence recovery after photobleaching 162
(FRAP) of the PKH26 dye. Briefly, an aperture on the light 163
path is used to selectively overexpose a small section of the 164
worm. The fluorescence recovery in the bleached region is 165
monitored by comparing the fluorescent intensity to that of 166
the Intensity in an unbleached section of the worm. 167

Paclitaxel (TAX) Encapsulation in OCL3 Micelles 168

TAX of 50 mg/ml in methanol was added into the micelle 169
solutions to obtain desired spiked TAX/polymer ratios. The 170
mixture was stirred at 25°C for 20 min and transferred to dialysis 171
cassettes (MWCO 10,000, Pierce, Rockford, IL). Dialysis was 172
performed against DPBS (pH 7.4) for 2 h to remove methanol 173
and small residues of dissolved TAX, and the obtained TAX- 174
loaded micelles were separated from insoluble-free TAX aggre- 175
gates by extrusion through a 10 ml thermobarrel extruder 176
(Northern Lipids, Vancouver, Canada) fitted with 0.65 μ m 177
filtering membranes (Millipore, Bedford, MA), and further 178
purified by filtration through 0.45 μ m Fischerbrand MCE filter 179
(Fisher Scientific). The preparation of TAX-encapsulated OCL3 180
micelles is illustrated in Fig. 1a. As an alternative method, TAX 181
was mixed with OCL3 polymer in chloroform solution before 182
micelle formation. The TAX-loaded micelles were then 183
obtained as described in “Preparation of OCL3 Polymeric 184
Micelles by cosolvent/Evaporation Method” followed by dialy- 185
sis and extrusion. 186

HPLC Assay Development and Validation 187

A Waters HPLC system (Waters, Milford, MA) equipped 188
with a 1525 Binary HPLC pump, a symmetry® reverse-phase 189
 C_{18} 5.0 μ m column (4.6 \times 150 mm), and a 2487 Dual λ 190
absorbance UV detector was used for TAX quantification. A 191
series of 1:2 TAX dilutions in acetonitrile ranging from 0 to 192
0.25 mg/ml were pre-mixed with equal volume of 0.25 mg/ml 193
docetaxel in acetonitrile as internal standard. The solutions 194
were filtered through 0.45 μ m filter followed by injection into 195
HPLC system. A mobile phase of 58% H₂O, 42% acetonitrile 196
at a flow rate of 1 ml/min was applied. TAX was detected and 197
quantified at UV 220 nm. The standard curve by plotting the 198
ratio of AUC of TAX and docetaxel was established, and the 199
linear range, intra-day and inter-day coefficient of variance 200
(CV), lower limit of detection (LLOD), lower limit of 201
quantification (LLOQ), assay accuracy and recovery (by 202
testing with 3, 10, and 40 μ g/ml TAX solution using the 203
standard curve) were calculated. To use the validated HPLC 204
assay to determine the TAX loading capacity and efficiency 205

206 in OCL3 micelles, TAX-loaded micelles were pre-mixed
 207 with equal volume of 0.25 mg/ml docetaxel in acetonitrile,
 208 and acetonitrile in equal volume to the mixture was further
 209 added, followed by the HPLC analysis using the standard
 210 curve described above. TAX loading capacity and efficiency
 211 were calculated based on the following expressions:

$$\text{TAX loading capacity} = \frac{\text{mass of TAX encapsulated in micelles/}}{\text{mass of OCL3 polymeric micelles}}$$

$$\text{TAX loading efficiency} = \frac{\text{mass of TAX encapsulated in micelles/}}{\text{mass of initially added TAX}}$$

217 **Thermal Analysis**

218 Thermal tests of OCL3 micelles were performed by
 219 differential scanning calorimetry (DSC) using a Differential
 220 Scanning Calorimeter 2920 (TA instruments, New Castle, DE).

221 TAX-loaded OCL3 worm micelles were lyophilized
 222 before the analysis. DSC thermograms of OCL3-TAX
 223 mixture (either in bulk before TAX loading or in lyophilized
 224 form after TAX loading) and OCL3 alone were then
 225 obtained by heating in sealed standard aluminum pans (TA
 226 instruments) from 25 to 100°C at a rate of 10°C/min followed
 227 by air cool and reheating to 100°C at the same rate.

228 **Micelle Stability and Paclitaxel Release Studies**

229 Both worm-like and spherical micelles (10 mg/ml), either
 230 drug-loaded or free, were stored at 4°C for 1 month or
 231 subjected to one-time freeze-thawing cycle. Then, the
 232 particle size was measured by DLS and the morphology was
 233 tested by fluorescent microscopy. TAX-loaded micelles were
 234 also examined for drug leakage potentially caused by storage
 235 or freeze-thawing cycles by centrifugation at 3,000 rpm for 5
 236 min to precipitate the TAX that may have diffused out. The
 237 supernatant was then mixed with acetonitrile and internal
 238 standard docetaxel for HPLC analysis.

239 Further, a dialysis method was employed to evaluate the
 240 *in vitro* release of TAX from OCL3 micelles. TAX-loaded
 241 worm-like and spherical micelles at a TAX concentration of
 242 40 µg/ml were added to the dialysis cassettes and dialyzed at
 243 37°C against DPBS of pH 6.8 and pH 7.4. At certain time
 244 points, the release medium was sampled and fresh DPBS was
 245 added to maintain the volume. The sampled medium was
 246 lyophilized and redissolved in chloroform. The insoluble
 247 buffer salt was removed by filtration. Chloroform was
 248 evaporated then and the remaining sample was re-dissolved
 249 in acetonitrile and subjected to aforementioned HPLC
 250 analysis.

251 **Cytotoxicity Assay**

252 TAX-loaded and drug-free micelles at serial dilutions were
 253 prepared per above. For comparison, 12 mg/ml TAX in ethanol
 254 was mixed with equal volume of Cremophor® EL followed by
 255 sonication for 30 min. The obtained Cremophor EL TAX was
 256 diluted with DPBS to obtain desired TAX concentrations.

257 Human lung-derived carcinoma cells A549 were grown
 258 in F12 Ham media supplemented with 10% fetal bovine
 259 serum and 100 U/ml penicillin and 100 µg/ml streptomycin at

37°C, 5% CO₂ to 60–70% confluence. A549 cells (50,000 cell/ml)
 were seeded in 96-well plates at 5,000 cells per well and
 cultured for 24 h to allow attachment. The medium was then
 exchanged and 100 µl of different tested formulations (free
 worm-like and spherical OCL3 micelles, Cremophor EL, free
 drug, TAX-loaded worm-like and spherical micelles, and
 Cremophor EL TAX) was added. As control, 100 µl of DPBS
 was added to cells not exposed to those formulations. After
 37°C, 5% CO₂ incubation for 72 h, the media were discarded,
 and 100 µl/well F12 Ham medium and 11 µl/well of 5 mg/ml
 MTT solution in DPBS was added. The plates were incu-
 bated at 37°C for 3 h and the media were removed again. The
 intracellular metabolized product MTT formazan was re-
 trieved by addition of 100 µl/well DMSO and incubation at
 room temperature for 5 min. The plates were read at 550 nm,
 and the cell viability was calculated as (reading of wells with
 cells exposed to tested formulations—reading of blank wells)/
 (reading of wells with cells exposed to DPBS—reading of
 blank wells).

279 **Data Analysis**

280 All data that require non-linear regression analysis were
 281 processed using GraphPad Prism (Version 4.03, GraphPad
 282 Software, San Diego, CA). The contour length distribution of
 283 OCL3 worm-like micelles was fit by Gaussian distribution,
 284 TAX and the carrier cytotoxicity assay on A549 cells was fit
 285 by sigmoid dose-response curve equation.

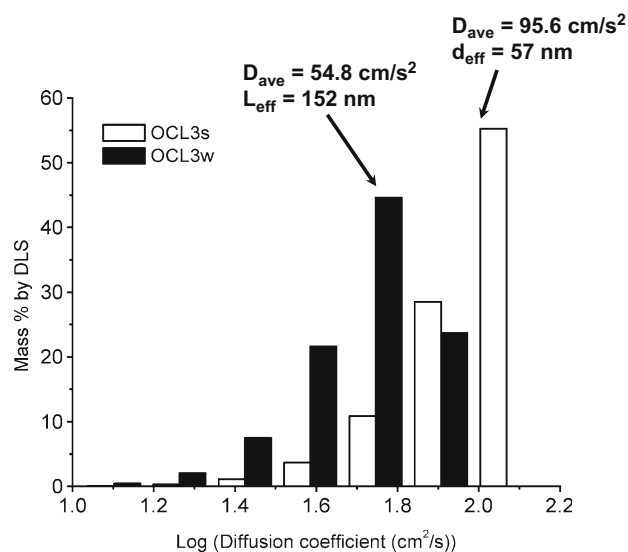


Fig. 2. Size and diffusion analysis of OCL3 micelles. The average diffusion coefficient distribution, and the calculated effective hydrodynamic size (diameter or length) of worm-like (before sonication) and spherical (after sonication) micelles were measured by DLS. The calculation of effective length of worm-like micelles is based on Stokes-Einstein equation: $D = kT / (2\pi\eta L_{eff})$ for worms (43) and $D = kT / (3\pi\eta d_{eff})$ for spheres, where D is the diffusion coefficient, k is the Boltzmann constant (1.38×10^{-23} J/K), T is the temperature (25°C), η is the viscosity of the solution (1.02 mPa·s from DLS), and d_{eff} is the hydrodynamic radius multiplied by 2

Micelles of Different Morphologies—Advantages of Worm-like Filomicelles of PEO-PCL in Paclitaxel Delivery

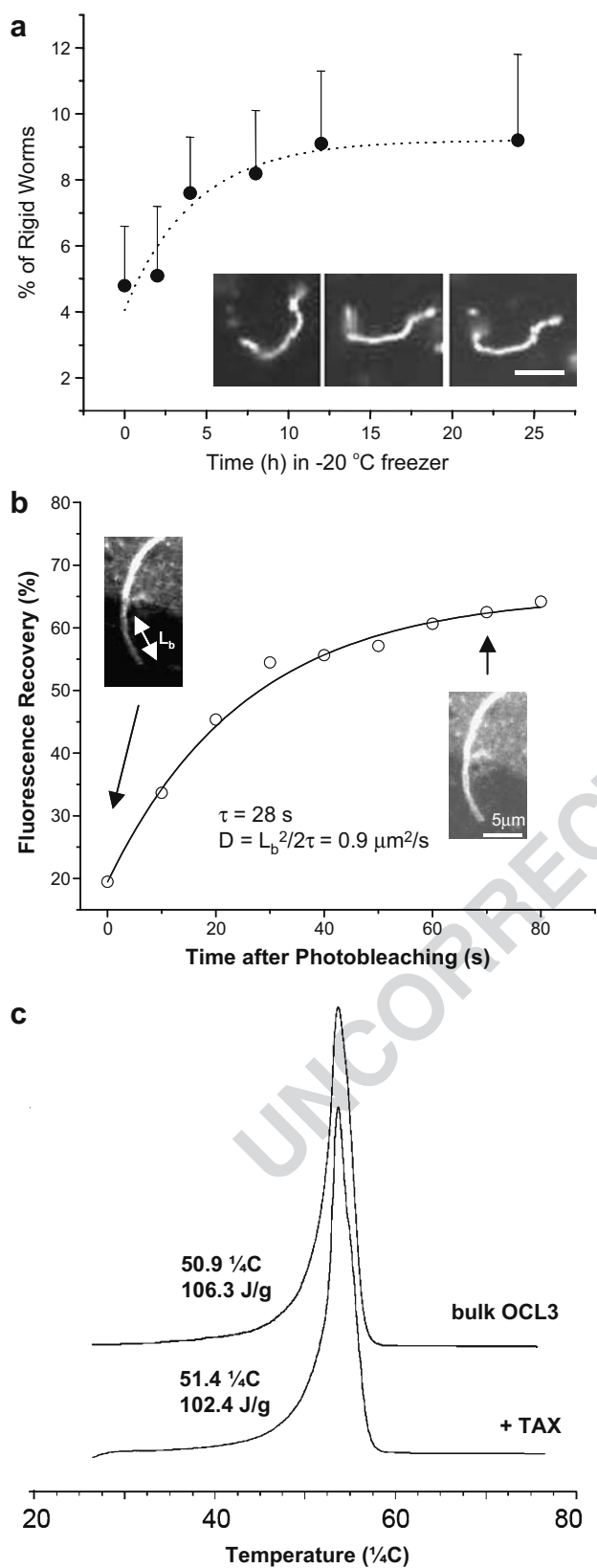


Fig. 3. Thermal and crystallinity analysis of OCL3 micelles. **a** Fluorescence recovery after photobleaching (FRAP) curve on OCL3 worms: A manual aperture in the light path was used to overexpose a small end section of the worm. The intensity in the bleached section was compared to that of a similar length of the worm in the unbleached section to normalize for bleaching during imaging. The FRAP data were fitted to an exponential recovery curve: Recovery % = $A(1 - e^{-t/\tau})$ (where A is the maximum recovery percentage and t is the time for recovery) to obtain an average recovery time constant $\tau \sim 28$ s. The 1-D diffusivity of the PKH26 dye was calculated from $D = L_b^2/2\tau$ where L_b is the length of the bleached region, and τ is the recovery time constant. $D \sim 0.9 \mu\text{m}^2/\text{s}$. **b** Percentage of rigid OCL3 worm-like micelles with possible crystallized cores over 12 h incubation at -20°C either in a 50% glycerol solution or pure water, after heating to 60°C and cooling to 30°C . The inset figures show frames in several different time points from sample rigid worms that were formed in glycerol. Scale bar 5 μm . **c** DSC thermogram ranging from 25 to 80°C of OCL3 polymer alone and TAX-OCL3 mixture

RESULTS

286

OCL3 Filomicelles are Fluid and can Fission to Spheres

287

A simple physicochemical measure of aggregate stability for strongly segregating amphiphiles is the critical micelle concentration (CMC), which is expected to be exponential in the length of the hydrophobic block (36). Based on a CMC of 1.2 $\mu\text{g}/\text{ml}$ for a sphere-forming OCL copolymer, EO₄₄-CL₂₁ (37), we estimate an immeasurably small CMC for our OCL3 copolymer EO₁₁₀-CL₅₈ of less than 1 fg/ml (i.e. $\text{CMC}_{\text{OCL3}} \sim [1.2 \mu\text{g}/\text{ml}]^{58/21}$). For later comparison, Cremophor EL reportedly has a $\text{CMC}_{\text{CremEL}} \sim 90 \mu\text{g}/\text{ml}$. For OCL3, micellar assemblies are clearly the predominant form in any aqueous solution. Moreover, since molecular exchange rates between micelles scale inversely with CMC, these low-CMC micelles can be considered kinetically trapped or frozen—without implying glassiness or crystallinity. OCL3’s weight fraction of ~ 0.43 for the hydrophilic PEO block drives assembly of most of the copolymer into worm-like and flexible filomicelles as observed by fluorescence microscopy after adding hydrophobic fluorescent dyes (Fig. 1b, inset). The average contour length of spontaneously assembled OCL3 filomicelles was calculated from measurement of at least 50 filomicelles, and as shown in Fig. 1b, most of the filomicelles are 6–7 μm , with some filomicelles as long as 14 μm .

288

289

290

291

292

293

294

295

296

297

298

299

300

301

302

303

304

305

306

307

308

309

Extrusion of worm-like filomicelles at high pressures and flow rates through nanoporous filters has been used to controllably reduce their length (13), but in order to convert to spherical micelles—simply and quantitatively—we exposed the filomicelles to robust sonication for several minutes. Diffusion coefficients (D_{ave}) were then measured by dynamic light scattering (DLS), and after sonication the effective hydrodynamic diameter was ~ 57 nm (Fig. 2). This is similar to previous ~ 60 nm estimates for the OCL3 filomicelle diameter of core plus corona as based on cryo-TEM (13). Prior to sonication, the measured D_{ave} proves significantly smaller and yields only a crude approximation for a larger effective size, but more important is the minimal overlap of the two distributions for D_{ave} . The 22% overlap suggests that a small fraction at most of the pre-sonicated

310

311

312

313

314

315

316

317

318

319

320

321

322

323

324

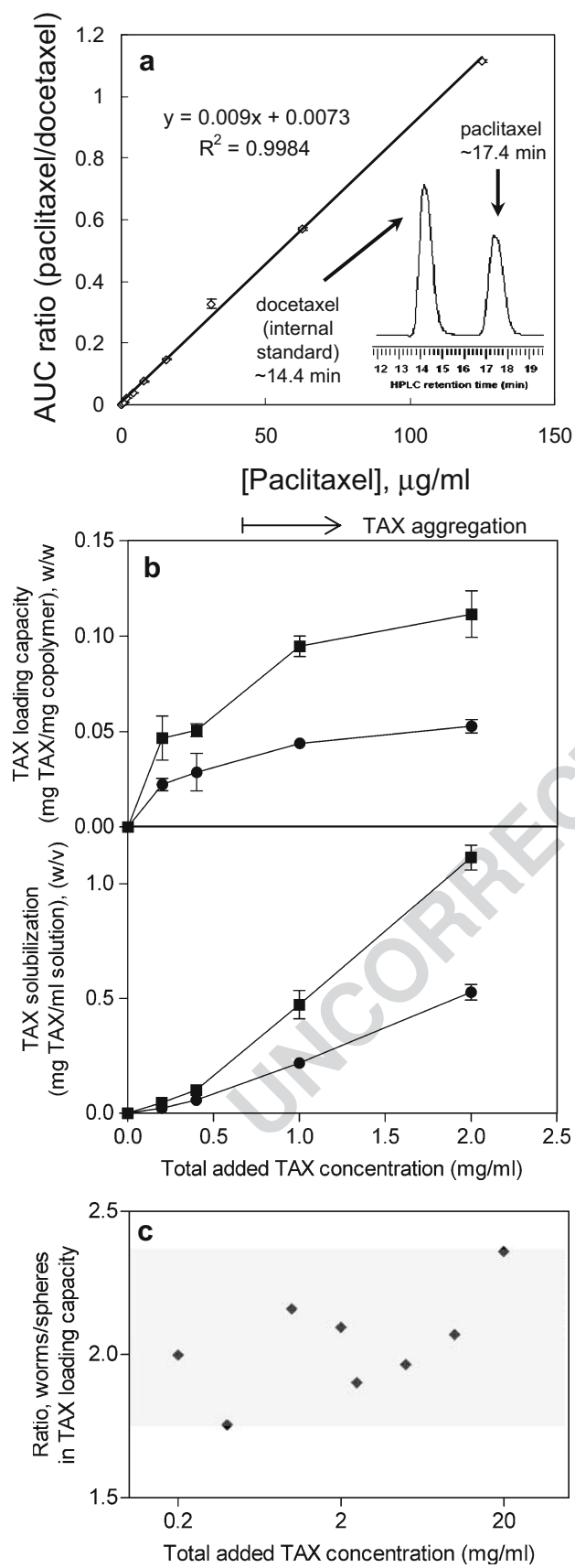


Fig. 4. HPLC-UV assay for paclitaxel (TAX) encapsulation. **a** Plot of HPLC-UV-determined area-under-curve (AUC) ratio between TAX and docetaxel vs TAX concentration. *Inset* shows the HPLC-UV spectrum of docetaxel (as internal standard) and paclitaxel (TAX). **b** TAX loading capacity (*upper panel*, defined as mg TAX loaded per milligram micelle) and solubilization (*lower panel*, defined as mg TAX loaded per milliliter aqueous solution) with OCL3 micelles when total added TAX:OCL3 micelle (w/w)=1:5; **c** ratio between TAX loading capacity with OCL3 worms and spheres at different conditions: Total added TAX:OCL3 micelle (w/w) was fixed at 1:5 while OCL3 concentration varied when added TAX concentration ≤ 2 mg/ml, and OCL3 micelle concentration was fixed at 10% (w/v) when added TAX concentration > 2 mg/ml

sample consists of spherical micelles. Worm-like filomicelles therefore predominate in freshly prepared OCL3 samples.

In bulk, PCL is a crystalline polymer at room temperature with melting in the range of 40–60°C (38), but past studies of PEO-based diblock copolymers in bulk suggest that PEO crystallization dominates in the same temperature range and frustrates crystallization of the connected block (38). For example, the diblock PEO-polyethylene (PE) in bulk is 70% PEO and only 10% crystalline (PE). On the other hand, dilution of filomicelles into water will generally hydrate and dissolve any crystallinity in the PEO corona. We had previously reported that OCL filomicelles appear as flexible as worm-like micelles made from non-crystalline and non-glassy diblock copolymers (e.g. PEO-polybutadiene), which implies a fluid core of PCL (30,39). However, our interest in loading and storage here involved freezing for an extended time, which are conditions that favor crystallization.

A very small fraction of the OCL3 filomicelles are inflexible coils as identified by end-to-end fluctuation $< 5\%$ of the average end-to-end distances relative to the more fluid-like and flexible filomicelles (Fig. 3a). Freezing in glycerol gave up to 10% of the bent but crystalline-behaving worm-like micelles (Fig. 3a). The core fluidity of the dominant population of flexible filomicelles was subsequently estimated by fluorescence recovery after photobleaching (FRAP) studies of immobilized filomicelles (Fig. 3b). The average recovery time for four different worms was ~ 30 s, which is similar to that observed in PBD cores of worm-like micelles with a similar molecular weight (40). The fast recovery rate in FRAP and the minor percentage of rigid worm micelles indicate a highly fluid PCL core, which would tend to favor loading and retention of hydrophobic drugs such as paclitaxel (TAX). Fluidity also provides a basis for filomicelle flexibility, which might allow these long micelles to reptate into diseased tissues, including tumors, despite their micron-scale length.

Before examining TAX loading of filomicelles and spheres in dilute solution, we examined the bulk melting of OCL3 with or without TAX using differential scanning calorimetry (DSC). A melting onset temperature near 51°C (Fig. 3c) is consistent with PEO and/or PCL crystallization, and the finding that TAX exerted no significant effect on melting temperature indicates a relative absence of disruptive interactions between the drug and the copolymer. Assuming the melting is attributable predominantly to PEO crystallization, as cited above (41), we estimate PEO crystallinity of 81% from the measured endotherm peak area (106.3 J/g without TAX), the heat of fusion for pure PEO (~ 300 J/g) (41), and the f_{EO} of OCL3. With the presence of TAX, there

325
326
327
328
329
330
331
332
333
334
335
336
337
338
339
340
341
342
343
344
345
346
347
348
349
350
351
352
353
354
355
356
357
358
359
360
361
362
363
364
365
366
367
368
369
370
371
372

Micelles of Different Morphologies—Advantages of Worm-like Filomicelles of PEO-PCL in Paclitaxel Delivery

Table I. Validation of HPLC-UV Assay for Paclitaxel, Using Docetaxel as the Internal Standard

| | Values |
|-------|------------------------------|
| t1.2 | |
| t1.3 | Linear range 0.5–125 µg/ml |
| t1.4 | Intra-day CV <15%, max 12.3% |
| t1.5 | Inter-day CV <15%, max 14.4% |
| t1.6 | Baseline noise ~0.0001 AU |
| t1.7 | LLOD 0.5 µg/ml |
| t1.8 | LLOQ 1.0 µg/ml |
| t1.9 | Accuracy 100.2±7.8% |
| t1.10 | Recovery 101.7±6.1% |

is no apparent decrease of crystalline PEO (79%) in bulk OCL3 (102.4 J/g with TAX), suggesting that TAX interaction with the copolymer is negligible.

Paclitaxel Integration into OCL3 Spheres and Filaments

TAX was then loaded into dilute micelles, and HPLC analysis was used to characterize the loading properties. An internal standard, docetaxel, was added in fixed amount to minimize variability (Fig. 4a; Table I). The lower limit of detection (LLOD) and lower limit of quantification (LLOQ) were as low as 0.5 and 1 µg/ml, and both the intra-day and inter-day coefficients of variance (CV) were less than 15%. An accuracy of 100.2±7.8% (n=6) and a recovery of 101.7±6.1% (n=6), were also obtained.

Loading of TAX before or after micelle formation showed no significant difference in capacity or efficiency (not shown). Figure 4b shows the TAX loading capacity and final concentration when TAX was initially added in a fixed 1:5 w/w ratio to micelles. Increasing TAX from 0.2 to 2 mg/ml (OCL3 1–10 mg/ml) increased both the loading capacity of TAX and the final solubilized TAX. Compared to spheres, OCL3 filomicelles showed about 2-fold greater loading capacity and at all concentrations (Fig. 4c).

Up to 10% w/v polymer concentration, with TAX varied from 2.5 to 5 mg/ml, the loading capacity for TAX increased, although the w/w loading was higher for 5% polymer. Further increases of added TAX up to 20 mg/ml led to a decrease in TAX solubilization regardless of morphology; this is probably due to the well-known aggregation of TAX at extremely high concentrations. The highest TAX solubilization obtained in the studies of filomicelles to date was 3 mg/ml, which is about 10,000-fold higher than natural TAX solubility in aqueous buffer [0.3 µg/ml, (18)]. Drug loading efficiency defined as (loaded drug/added drug) is

Table III. Loading Efficiency of TAX into OCL3 Spherical and Worm-like Micelles at 10% (w/v) Fixed OCL3 Micelle Concentration

| | Total TAX Concentration (mg/ml) | | | |
|---------|---------------------------------|------|------|------|
| | 2.5 | 5 | 10 | 20 |
| Spheres | 0.34 | 0.30 | 0.09 | 0.03 |
| Worms | 0.64 | 0.59 | 0.18 | 0.06 |

Loading Efficiency mass of solubilized TAX/mass of initially added TAX

tabulated in Tables II, III, and IV and consistently appears 2-fold higher with filomicelles than with spherical micelles.

In addition to the encapsulation capacity studies, an identical DSC thermogram for lyophilized OCL3–TAX mixture after encapsulation (not shown) with that of OCL3–TAX mixture in bulk (Fig. 3c) again verifies the unchanged melting temperature and the fusion heat of OCL3 copolymer. This further demonstrates the absence of interactions of TAX with its excipient during the encapsulation process.

Stability and In Vitro Release

Possible effects of storage, drug loading and extrusion on morphological changes of filomicelles were examined by DLS and fluorescence imaging. Fig. 5a shows that (1) both shapes of micelle are morphologically stable in 4°C storage for up to 1 month; (2) TAX integration does not affect micelle size, which is probably because the small loaded mass of TAX cannot swell the relatively large cores within micelles; (3) spherical micelles made by sonicating worm-like filomicelles show no further size change after extrusion whereas filomicelles become smaller. The latter result was confirmed by contour length measurement under fluorescence microscopy (Fig. 1b), which shows that extrusion left-shifts and narrows the length distribution from 6.6–7.3 µm (95%) to 5.6–6.1 µm.

Stability of TAX loading within OCL3 micelles was evaluated after 1 month of storage. Fig. 5b shows that when TAX-loaded micelles of either morphology were either maintained in fluid form at 4°C or else frozen (and perhaps crystalline) at –20°C, no significant leakage or precipitation of TAX could be detected. As emphasized above and further below, the filomicelle carriers are clearly stable under harsh treatments. For application, freezing has the advantage in slowing hydrolytic degradation of PCL (30).

In addition, filomicelles were subjected to freeze–thaw cycles (–20°C) as another potentially disruptive operation

Table II. Loading Efficiency of TAX into OCL3 Spherical and Worm-like Micelles When Initial Added TAX:OCL3 Micelle (w/w)=1:5

| | Total TAX Concentration (mg/ml) | | | | |
|---------|---------------------------------|------|------|------|------|
| | 0.2 | 0.4 | 1 | 2 | 20 |
| Spheres | 0.11 | 0.14 | 0.22 | 0.26 | 0.03 |
| Worms | 0.23 | 0.25 | 0.47 | 0.56 | 0.06 |

Loading Efficiency mass of solubilized TAX/mass of initially added TAX

Table IV. Loading Efficiency of TAX into Worm-Like OCL3 Micelles at 5 and 10% (w/v)

| | Total TAX Concentration (mg/ml) | | |
|----------|---------------------------------|------|------|
| | 2.5 | 5 | 10 |
| 5% Worm | 0.44 | 0.49 | 0.17 |
| 10% Worm | 0.64 | 0.59 | 0.18 |

Loading Efficiency mass of solubilized TAX/mass of initially added TAX

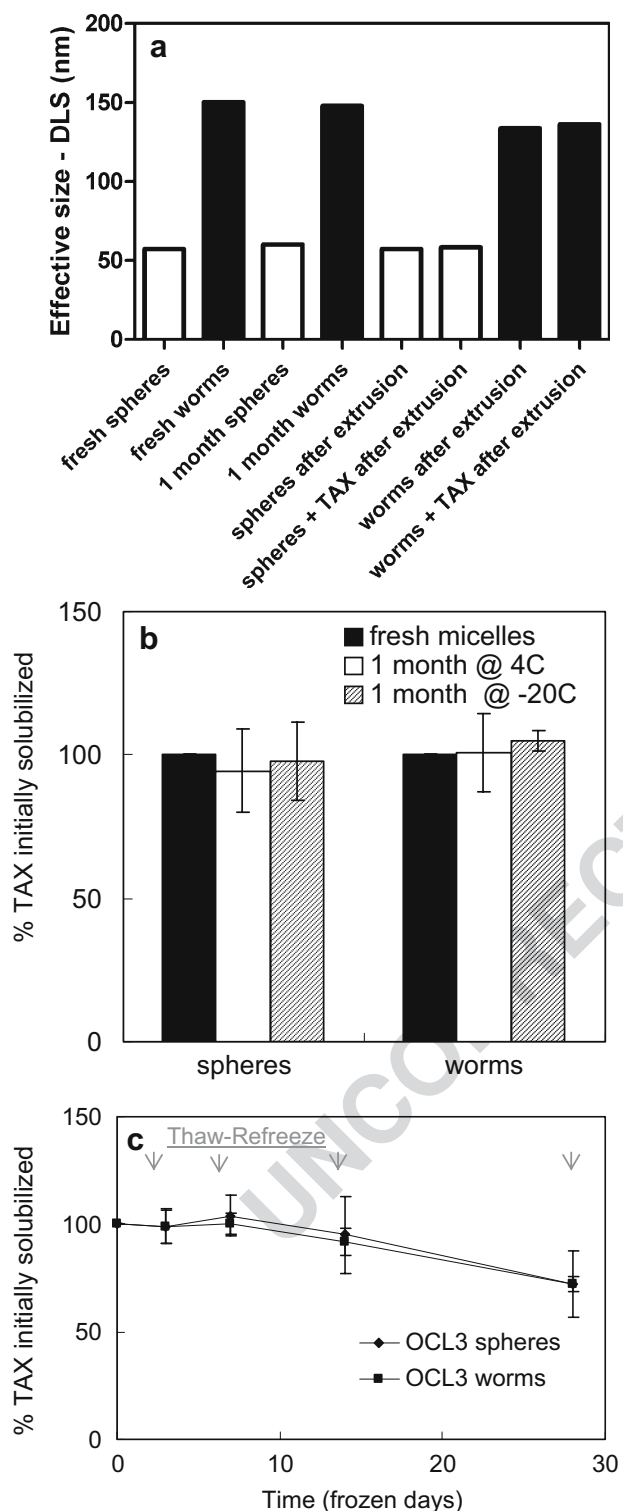


Fig. 5. Effect of extrusion, TAX loading, freeze-thawing and storage on micelle morphology and leakage of encapsulated drug. **a** Effect of extrusion, TAX loading and 1 month storage on the micelle effective size, determined by DLS; **b** effect of 1 month storage at 4 and -20°C on TAX leakage from micelles; **c** effect of multiple freeze-thawing cycles at -20°C on TAX leakage from micelles

that multiple freeze-thaw cycles lead to drug leakage from both morphologies. TAX-loaded OCL3 micelles were frozen at day 0, then thawed at day 3 for the test and re-frozen, which was repeated at day 7, 14, 28. By the fourth cycle, the TAX retained in the micelle cores decreased to about 70% of initial loading. The reasons are not yet as clear as the practical implications.

Release *in vitro* at 37°C was also studied at pH 7.4, per normal tissue pH, and also at pH 6.8 to mimic the slightly acidic cancerous tissue environment (29,35). As the PCL in OCL3 is known to undergo accelerated hydrolysis at acidic pH (30), TAX release rates proved to be 40% faster at lower pH but similar for both morphologies. This indicates that pH rather than shape is the more critical parameter to control drug release.

Enhanced Cytotoxicity of TAX Released from OCL3 Micelles

Human lung carcinoma-derived A549 cells were used in cytotoxicity assays of both micelles as empty carriers and also as TAX-loaded carriers. The *in-clinic*, commercial TAX formulation with Cremophor EL was also included as a benchmark. Excipient toxicity is critically important to assessing the specific anticancer effect of TAX, and so for ease of comparison we therefore calculate the equivalent TAX concentration; for example, 0.8 mg TAX corresponds to about 1 g Cremophor EL (see “MATERIALS AND METHODS”). Based on such analyses, Cremophor EL shows a significant cytotoxic effect at only 2–3 $\mu\text{g}/\text{ml}$ equivalents of TAX (Fig. 6a). In contrast, the OCL3 polymeric micelles showed no obvious toxicity up to almost 100 $\mu\text{g}/\text{ml}$ TAX equivalents. Identifying the dose of excipients at which 80% of cells are still alive (‘inhibition constant’ IC80) as a parameterization of toxicity and then converting to cytotoxic carrier doses yields $\text{IC80}_{\text{CremEL}}=120 \mu\text{g}/\text{ml}$ for Cremophor EL, which appears only slightly higher than $\text{CMC}_{\text{CremEL}}\approx 90 \mu\text{g}/\text{ml}$ and implies the aggregate form of Cremophor EL is toxic (Fig. 6b). For both filomicelles and spheres, $\text{IC80}_{\text{OCL3-micelle}}=1,500 \mu\text{g}/\text{ml}$, which is about 13-orders of magnitude higher than CMC_{OCL3} and suggests mechanisms of cell death such as micellar poration previously discussed for PEO-PCL polymersomes (30). Regardless, the 13-fold difference indicates, of course, that OCL3 polymeric micelles are much safer excipients.

TAX formulations with the various carriers consistently improve cytotoxicity relative to delivery of free drug. While Fig. 6c shows that TAX-loaded Cremophor EL begins killing cells in the nanogram/milliliter range of TAX and kills nearly all cells at $[\text{TAX}]\approx 10\text{--}100 \mu\text{g}/\text{ml}$ (Fig. 6a), the Cremophor EL excipient rather than TAX is clearly responsible for a significant fraction of the cytotoxicity. On the other hand, TAX-loaded OCL3 micelles exhibit similar cytotoxicity in the 10 ng/ml range, killing more than 35% A549 cancer cells. Importantly, the anticancer effects of TAX-loaded OCL3 micelles throughout the tested concentrations were all attributed to the drug activity, instead of the toxicity from the carriers. The fitted sigmoid dose-response curve showed that the IC50 -cytotoxicity of TAX-loaded OCL3 micelles (at $\sim 25 \text{ nM}$) was 13-fold more potent than free TAX (321 nM for A549 cells) and also 5-fold better than Cremophor EL TAX (Fig. 6d). Both worm-like filomicelles and spherical

relevant to storage. After a single cycle, there was no significant change in the length distribution shown in Fig. 1b or in TAX retention (Fig. 5c). However, the latter plot shows

Micelles of Different Morphologies—Advantages of Worm-like Filomicelles of PEO-PCL in Paclitaxel Delivery

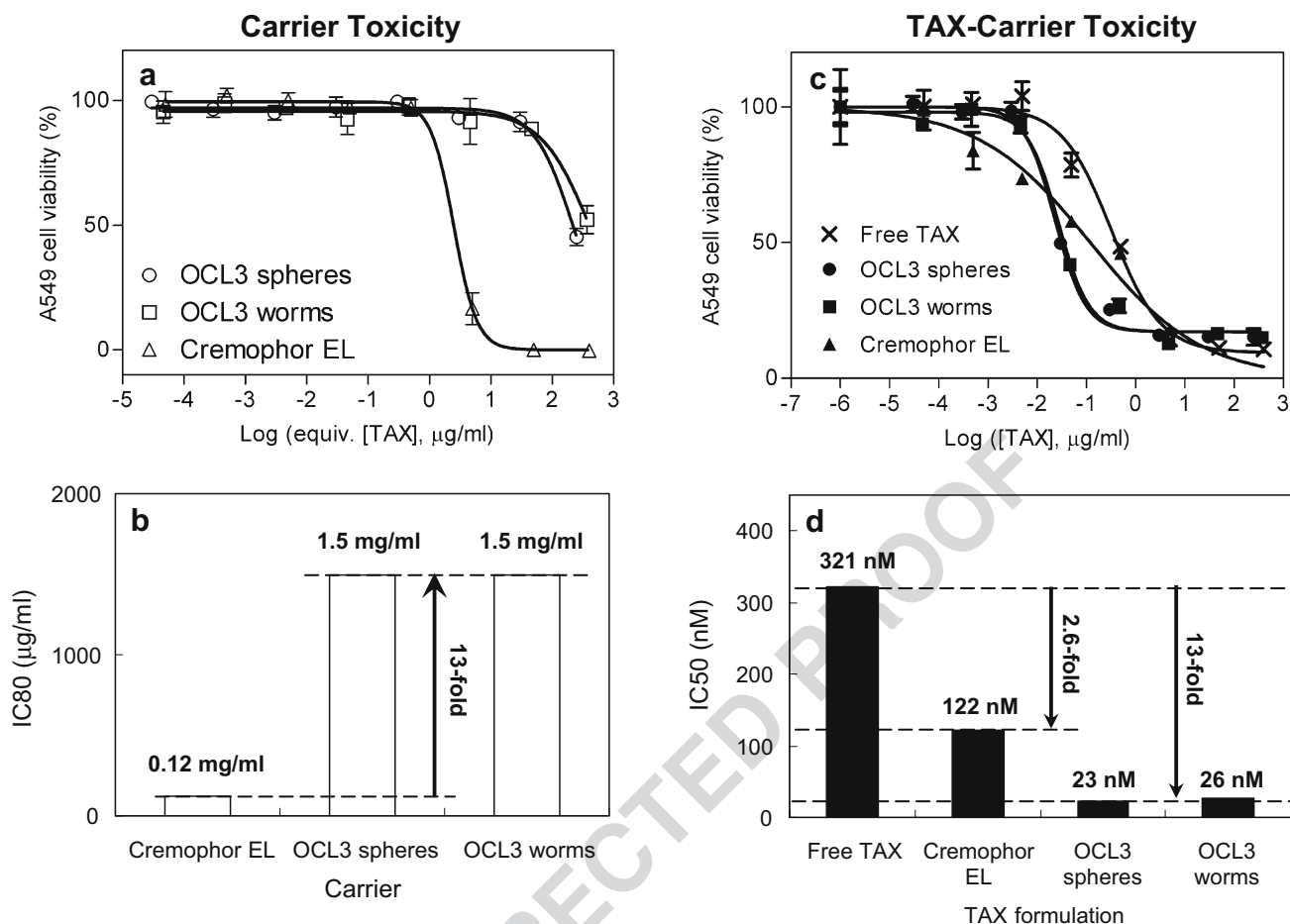


Fig. 6. Cytotoxicity study and IC₅₀ evaluation of TAX-loaded micelles on A549 human lung carcinoma cells. **a** Cytotoxicity of excipient only (OCL3 spheres, worms, and Cremophor EL) on A549 cells; **b** comparison of the excipient concentration at which 20% cells were killed (IC₈₀); **c** cytotoxicity of different TAX formulations on A549 cells; **d** comparison of IC₅₀ of different TAX formulations. Sigmoid dose-responsive equation : $Y = \text{Bottom} + (\text{Top} - \text{Bottom}) / (1 + 10^{((\text{LogIC}_{50} - X) * \text{HillSlope}))}$, where X is the logarithm of TAX concentration, Y is the response and starts at bottom and goes to top, and HillSlope is the slope for the linear dropping region in the sigmoid curve

503 micelles showed the same enhanced cytotoxicity. Since OCL3
 504 filomicelles have a higher drug loading capacity compared to
 505 spherical micelles and otherwise display similar stability and
 506 efficacy as spherical micelles, the filomicelles seem an attractive
 507 alternative for the emerging tests of parenteral delivery (13).

508 **DISCUSSION**

509 TAX is a widely used chemotherapeutic for cancer
 510 treatment, but its poor water solubility [0.3 $\mu\text{g/ml}$ at 25°C
 511 (18)] requires clinical use of solubilizers. Cremophor EL is
 512 widely used but has side-effects and limitations that are clear
 513 both in these simple studies and in the clinic. PEO-based
 514 spherical micelles made from amphiphilic diblock copoly-
 515 mers have been explored as an alternative type of carrier
 516 system to load hydrophobic drugs and dyes into the
 517 hydrophobic cores, and our recent studies have focused in
 518 some detail on assembly and properties of worm-like
 519 filomicelles (30–34). The needed copolymers are typically
 520 composed of ~0.4–0.5 weight fraction of hydrophilic PEO
 521 polymer and yield flexible but highly stable filamentous

micelles that surprisingly increase the circulation time in the
 blood stream relative to spheres. Here we showed the
 filomicelles -generally have a fluid core (Fig. 3), which favors
 integration of drugs into their hydrophobic cores, and we
 then examined the drug loading capacity and various other
 performance aspects of PEO-PCL worm-like filomicelles for
 comparison to spheres generated from the same filomicelles
 by sonication. Loading advantages are clear (Fig. 4b,c,
 Tables II, III, and IV), and some insight is gained from
 simple calculations of volume to surface area for spheres and
 cylinders. For spheres of radius r , volume/surface area =
 $(4/3 \pi r^3) / (4\pi r^2) = r/3$, whereas for cylinders of length L ,
 volume/surface area = $(\pi r^2 L) / (2\pi r L) = r/2$. If micellar
 area is thus held constant for a given mass of copolymer in
 solution, then the filomicelles are expected to carry more
 hydrophobic drug than spheres by a ratio of $(r/2 - r/3) /$
 $(r/3) = 50\%$. The bigger difference of ~100% found here
 certainly highlights the advantageous loading of drugs into
 filomicelles. Furthermore, the maximum concentration of
 solubilized TAX reached 3 mg/ml, placing filomicelles just
 below Cremophor EL (marketed as formulations containing
 6 mg/ml TAX) but among the top micelle-based TAX

544 delivery systems that usually enhance TAX solubility to 1–2
545 mg/ml (18,21,23–25,42).

546 Although filomicelles appear novel and were perhaps
547 even overlooked in past formulations that relied on sonica-
548 tion, PEO-PCL block copolymer has been widely explored
549 for drug delivery applications in the past. It consists of FDA-
550 approved PEO plus the approved and degradable polyester
551 PCL. We have previously found that hydrolytic degradation
552 of PCL predominates at the distal hydroxyl-end such that the
553 hydrophobic mass of PCL gradually decreases, increasing the
554 weight fraction of PEO and converting the worm-like
555 micelles towards spherical micelles (30). This process is
556 greatly accelerated by low pH, which also accelerates release
557 of TAX. On the other hand, degradation of PCL is
558 significantly limited at low temperatures of 4 and –20°C,
559 and the results here demonstrate stable storage of OCL3
560 filomicelle morphologies at these low temperatures for
561 a month (Fig. 5) without major complications from crystalliza-
562 tion (Fig. 3). While multiple freeze–thaw cycles leads to loss
563 of TAX for both worm-like and spherical micelles—as do
564 other harsh conditions in extrusion, sonication, and lyophiliza-
565 tion (not shown), only 1–2 cycles of freeze–thaw cycles
566 have no obvious effect. Care should nonetheless be taken
567 when preparing or storing TAX-loaded worm micelles.

568 Given the persistent circulation of filomicelles and
569 minimal accumulation in rat lung (21), specific targeting of
570 these novel morphologies to lung tumors should eventually
571 provide a clear indication of directed drug delivery possibil-
572 ities with filomicelles. Human lung cancer also continues to
573 account for a significant of all cancer deaths. With these
574 factors in mind as well as the intrinsic toxicity of Cremophor
575 EL (Fig. 6a,b), we examined the *in vitro* delivery by
576 filomicelles of TAX to A549 lung carcinoma cells, and we
577 find that the spherical micelles and filomicelles are both 13-
578 fold less toxic than Cremophor EL and, with loaded TAX,
579 about 5-fold more effective in delivering a cytotoxic dose
580 (Fig. 6c,d). Furthermore, since delivery of Cremophor EL is
581 not pH-sensitive, such an *in vivo* formulation will tend to be
582 less selective for tumors and further increase the risk of the
583 excipient toxicity to normal cells.

584 **CONCLUSION**

585 Taken together, OCL3 based filomicelles appear to
586 provide an excellent system for delivery of hydrophobic
587 drugs, with enhanced drug solubility compared to spherical
588 micelles but similar efficacy for a given dose of TAX.
589 Morphological changes thus did not adversely impact drug
590 release behavior and *in vitro* bioactivity. Future studies are
591 likely to include conjugation with targeting moieties towards
592 lung cancer cells and studies of *in vivo* tumor models with
593 parenteral administration. Morphological effects under these
594 more pathophysiological conditions clearly need to be
595 mapped out.

596 **ACKNOWLEDGEMENTS**

597 This study was supported by grants from NIH-NIBIB
598 and NSF-MRSEC.

REFERENCES

1. M. J. Vicent, R. Duncan. Polymer conjugates: nanosized 600
medicines for treating cancer. *Trends Biotechnol.* **24**:39–47 601
(2006). 602

2. A. Malugin, P. Kopeckova, and J. Kopecek. HEMA copolymer- 603
bound doxorubicin induces apoptosis in ovarian carcinoma cells 604
by the disruption of mitochondrial function. *Mol. Pharmacol.* 605
3:351–361 (2006). 606

3. Y. Luo, M. R. Ziebell, and G. D. Prestwich. A hyaluronic acid- 607
taxol antitumor bioconjugate targeted to cancer cells. *Bioma- 608*
cro-molecules. **1**:208–218 (2000). 609

4. L. E. van Vlerkenand, and M. M. Amiji. Multi-functional 610
polymeric nanoparticles for tumour-targeted drug delivery. 611
Expert Opin. Drug Deliv. **3**:205–216 (2006). 612

5. B. Liu, S. Jiang, W. Zhang, F. Ye, Y. H. Wang, J. Wu, and D. Y. 613
Zhang. Novel biodegradable HSAM nanoparticle for drug 614
delivery. *Oncol. Rep.* **15**:957–961 (2006). 615

6. V. P. Torchilin. Recent advances with liposomes as pharmaceu- 616
tical carriers. *Nat. Rev. Drug Discov.* **4**:145–160 (2005). 617

7. X. Guoand, F. C. Szoka Jr. Chemical approaches to triggerable 618
lipid vesicles for drug and gene delivery. *Acc. Chem. Res* **36**:335– 619
341 (2003). 620

8. F. Ahmed, R. I. Pakunlu, G. Srinivas, A. Brannan, F. Bates, M. L. 621
Klein, T. Minko, and D. E. Discher. Shrinkage of a rapidly 622
growing tumor by drug-loaded polymersomes: pH-triggered 623
release through copolymer degradation. *Mol. Pharmacol.* **3**:340– 624
350 (2006). 625

9. F. Ahmed, R. I. Pakunlu, A. Brannan, F. Bates, T. Minko, and 626
D. E. Discher. Biodegradable polymersomes loaded with both 627
paclitaxel and doxorubicin permeate and shrink tumors, inducing 628
apoptosis in proportion to accumulated drug. *J. Control. Release.* 629
116:150–158 (2006). 630

10. J. P. Xu, J. Ji, W. D. Chen, and J. C. Shen. Novel biomimetic 631
polymersomes as polymer therapeutics for drug delivery. *J.* 632
Control. Release. **107**:502–512 (2005). 633

11. Y. Bae, W. D. Jang, N. Nishiyama, S. Fukushima, and K. Kataoka. 634
Multifunctional polymeric micelles with folate-mediated cancer 635
cell targeting and pH-triggered drug releasing properties for 636
active intracellular drug delivery. *Mol. BioSyst.* **1**:242–250 637
(2005). 638

12. J. Wang, D. Mongayt, and V. P. Torchilin. Polymeric micelles 639
for delivery of poorly soluble drugs: preparation and anticancer 640
activity in vitro of paclitaxel incorporated into mixed micelles 641
based on poly(ethylene glycol)–lipid conjugate and positively 642
charged lipids. *J. Drug Target.* **13**:73–80 (2005). 643

13. Y. Geng, P. Dalhaimer, S. Cai, R. Tsai, M. Tewari, T. Minko, 644
and D. E. Discher. Soft filaments circulate longer than spherical 645
particles-shape effects in flow and drug delivery. *Nat. Nanotech.* 646
(2007) (in press). 647

14. X. Tong, J. Zhou, and Y. Tan. Liquid chromatography/tandem 648
triple-quadrupole mass spectrometry for determination of pac- 649
litaxel in rat tissues. *Rapid Commun. Mass Spectrom.* **20**:1905– 650
1912 (2006). 651

15. T. Y. Kim, D. W. Kim, J. Y. Chung, S. G. Shin, S. C. Kim, D. S. 652
Heo, N. K. Kim, and Y. J. Bang. Phase I and pharmacokinetic 653
study of Genexol-PM, a cremophor-free, polymeric micelle- 654
formulated paclitaxel, in patients with advanced malignancies. 655
Clin. Cancer Res. **10**:3708–3716 (2004). 656

16. S. C. Kim, J. Yu, J. W. Lee, E. S. Park, and S. C. Chi. Sensitive 657
HPLC method for quantitation of paclitaxel (Genexol in biolog- 658
ical samples with application to preclinical pharmacokinetics and 659
biodistribution. *J. Pharm. Biomed. Anal.* **39**:170–176 (2005). 660

17. L. M. Han, J. Guo, L. J. Zhang, Q. S. Wang, and X. L. Fang. 661
Pharmacokinetics and biodistribution of polymeric micelles of 662
paclitaxel with Pluronic P123. *Acta Pharmacol. Sin.* **27**:747–753 663
(2006). 664

18. O. Soga, C. F. van Nostrum, M. Fens, C. J. Rijcken, R. M. 665
Schiffelers, G. Storm, and W. E. Hennink. Thermosensitive and 666
biodegradable polymeric micelles for paclitaxel delivery. *J.* 667
Control. Release. **103**:341–353 (2005). 668

19. R. T. Liggins, W. L. Hunter, and H. M. Burt. Solid-state 669
characterization of paclitaxel. *J. Pharm. Sci.* **86**:1458–1463 (1997). 670

Micelles of Different Morphologies—Advantages of Worm-like Filomicelles of PEO-PCL in Paclitaxel Delivery

- 671 20. S. C. Kim, D. W. Kim, Y. H. Shim, J. S. Bang, H. S. Oh, S. Wan
672 Kim, and M. H. Seo. In vivo evaluation of polymeric micellar
673 paclitaxel formulation: toxicity and efficacy. *J. Control. Release.*
674 **72**:191–202 (2001).
- 675 21. S. Cheon Lee, C. Kim, I. Chan Kwon, H. Chung, and S. Young
676 Jeong. Polymeric micelles of poly(2-ethyl-2-oxazoline)-block-
677 poly(epsilon-caprolactone) copolymer as a carrier for paclitaxel.
678 *J. Control. Release.* **89**:437–446 (2003).
- 679 22. T. Meyer, D. Waidelich, and A. W. Frahm. Separation and first
680 structure elucidation of Cremophor EL-components by hyphen-
681 ated capillary electrophoresis and delayed extraction-matrix
682 assisted laser desorption/ionization-time of flight-mass spec-
683 trometry. *Electrophoresis.* **23**:1053–1062 (2002).
- 684 23. Y. Moand, L.Y. Lim. Preparation and *in vitro* anticancer activity
685 of wheat germ agglutinin (WGA)-conjugated PLGA nano-
686 particles loaded with paclitaxel and isopropyl myristate. *J.*
687 *Control. Release* **107**:30–42 (2005).
- 688 24. S. Q. Liu, Y. W. Tong, and Y. Y. Yang. Thermally sensitive micelles
689 self-assembled from poly(*N*-isopropylacrylamide-co-*N,N*-dime-
690 thylacrylamide)-*b*-poly(D,L-lactide-*c* *o*-glycolide) for controlled
691 delivery of paclitaxel. *Mol. BioSyst.* **1**:158–165 (2005).
- 692 25. J. Xie, C. H. Wang. Self-assembled biodegradable nanoparticles
693 developed by direct dialysis for the delivery of paclitaxel.
694 *Pharm. Res.* **22**:2079–2090 (2005).
- 695 26. G. Gaucher, M. H. Dufresne, V. P. Sant, N. Kang, D. Maysinger,
696 and J. C. Leroux. Block copolymer micelles: preparation,
697 characterization and application in drug delivery. *J. Control.*
698 *Release.* **109**:169–188 (2005).
- 699 27. F. Yoshii, D. Darwis, H. Mitomo, and K. Makuuchi. Cross-
700 linking of poly(beta-caprolactone) by radiation technique and its
701 biodegradability. *Radiat. Phys. Chem.* **57**:417–420 (2000).
- 702 28. R. T. Liggins, T. Cruz, W. Min, L. Liang, W. L. Hunter, and
703 H. M. Burt. Intra-articular treatment of arthritis with micro-
704 sphere formulations of paclitaxel: biocompatibility and efficacy
705 determinations in rabbits. *Inflamm. Res.* **53**:363–372 (2004).
- 706 29. Z. G. Gao, D. H. Lee, D. I. Kim, and Y. H. Bae. Doxorubicin loaded
707 pH-sensitive micelle targeting acidic extracellular pH of human
708 ovarian A2780 tumor in mice. *J. Drug Target.* **13**:391–397 (2005).
- 709 30. Y. Gengand, D. E. Discher. Hydrolytic degradation of poly
710 (ethylene oxide)-block-polycaprolactone worm micelles. *J. Am.*
711 *Chem. Soc.* **127**:12780–12781 (2005).
- 712 31. P. Dalhaimer, F. S. Bates, and D. E. Discher. Single molecule
visualization of stable, stiffness-tunable, flow-conforming worm
micelles. *Macromolecules.* **36**:6873–6877 (2003).
32. Y. Kim, P. Dalhaimer, D. A. Christian, and D. E. Discher.
Polymeric worm micelles as nano-carriers for drug delivery.
Nanotechnology. **16**:S484–S491 (2005).
33. Y. Geng, F. Ahmed, N. Bhasin, and D. E. Discher. Visualizing
worm micelle dynamics and phase transitions of a charged
diblock copolymer in water. *J. Phys. Chem., B Condens. Mater.*
Surf. Interfaces Biophys. **109**:3772–3779 (2005).
34. P. Dalhaimer, A. J. Engler, R. Parthasarathy, and D. E. Discher.
Targeted worm micelles. *Biomacromolecules.* **5**:1714–1719 (2004).
35. S. D. Webb, J. A. Sherratt, and R. G. Fish. Alterations in
proteolytic activity at low pH and its association with invasion: a
theoretical model. *Clin. Exp. Metastasis.* **17**:397–407 (1999).
36. K. Vijayanand, D. E. Discher. Block copolymer worm micelles
in dilution: mechanochemical metrics of robustness as a basis for
novel linear assemblies. *J. Polym. Sci., B, Polym. Phys.* **44**:3431–
3433 (2006).
37. L. Luo, J. Tam, D. Maysinger, and A. Eisenberg. Cellular
internalization of poly(ethylene oxide)-*b*-poly(epsilon-caprolactone)
diblock copolymer micelles. *Bioconjug. Chem.* **13**:1259–1265 (2002).
38. P. Skoglundand, A. Fransson. Continuous cooling and isother-
mal crystallization of polycaprolactone. *J. Appl. Polym. Sci.*
61:2455–2465 (1996).
39. V. Balsamo, C. U. de Navarro, and G. Gil. Microphase separation
vs crystallization in polystyrene-*b*-polybutadiene-*b*-poly(epsilon-
caprolactone) ABC triblock copolymers. *Macromolecules*
36:4507–4514 (2003).
40. Y. Geng, D. E. Discher, J. Justynska, and H. Schlaad. Grafting
short peptides onto polybutadiene-block-poly(ethylene oxide): a
platform for self-assembling hybrid amphiphiles. *Angew. Chem.,*
Int. Ed. Engl. **45**:7578–7581 (2006).
41. M. A. Hillmyerand, F. S. Bates. Synthesis and characterization
of model polyalkane-poly(ethylene oxide) block copolymers.
Macromolecules **29**:6994–7002 (1996).
42. J. H. Kim, K. Emoto, M. Lijima, Y. Nagasaki, T. Aoyagi, T. Okano,
Y. Sakurai, and K. Kataoka. Core-stabilized polymeric micelle as
potential drug carrier: increased solubilization of taxol. *Polym.*
Adv. Technol. **10**:647–654 (1999).
43. G. L. Li and J. X. Tang. Diffusion of actin filaments within a thin
layer between two walls. *Phys. Rev., E Stat. Nonlin. Soft Matter*
Phys. **69**:(2004).

AUTHOR QUERIES

AUTHOR PLEASE ANSWER ALL QUERIES.

- Q1. Please check table header provided.
- Q2. Table 2 was split into Tables 2, 3, and 4, and citations 2 A-C were changed to Tables 2, 3, and 4. Please check if appropriate.
- Q3. Please provide bibliographic update for reference item [13] once available.

UNCORRECTED PROOF